



Published in final edited form as:

*J Autoimmun.* 2018 June ; 90: 84–93. doi:10.1016/j.jaut.2018.02.004.

## Targeting CD6 for the treatment of experimental autoimmune uveitis

Lingjun Zhang<sup>1</sup>, Yan Li<sup>1</sup>, Wen Qiu<sup>1</sup>, Brent A Bell<sup>2</sup>, Nina Dvorina<sup>1</sup>, William M. Baldwin III<sup>1</sup>, Nora Singer<sup>3</sup>, Timothy Kern<sup>4</sup>, Rachel R Caspi<sup>5</sup>, David A Fox<sup>6</sup>, and Feng Lin<sup>1</sup>

<sup>1</sup>Department of Immunology, Cleveland Clinic, Cleveland, Ohio 44195, USA

<sup>2</sup>Cole Eye Institute, Cleveland Clinic, Cleveland, Ohio 44195, USA

<sup>3</sup>Department of Medicine and Pediatrics, MetroHealth Medical Center, Case Western Reserve University, Cleveland, Ohio 44106

<sup>4</sup>Department of Medicine and Ophthalmology, Case Western Reserve University, Cleveland, Ohio 44106, USA

<sup>5</sup>Laboratory of Immunology, National Eye Institute, National Institutes of Health, Bethesda, MD, USA

<sup>6</sup>Division of Rheumatology and Clinical Autoimmunity Center of Excellence, University of Michigan, Ann Arbor, MI 48109

### Abstract

**Objective**—CD6 is emerging as a new target for treating many pathological conditions in which T cells are integrally involved, but even the latest data from studies of CD6 gene engineered mice were still contradictory. To address this issue, we studied experimental autoimmune uveitis (EAU), a model of autoimmune uveitis, in wild-type (WT) and CD6 knockout (KO) mice.

**Methods**—After EAU induction in WT and CD6 KO mice, we evaluated ocular inflammation and compared retinal antigen-specific T-cell responses using scanning laser ophthalmoscopy, spectral-domain optical coherence tomography, histopathology, and T cell recall assays. Uveitogenic T cells from WT and CD6 KO mice were adoptively transferred into WT naïve mice to confirm the impact of CD6 on T cells. In addition, we immunized CD6 KO mice with recombinant CD6 protein to develop mouse anti-mouse CD6 monoclonal antibodies (mAbs) in which functional antibodies exhibiting cross-reactivity with human CD6 were screened and identified for treatment studies.

**Results**—In CD6 KO mice with EAU, we found significantly decreased retinal inflammation and reduced autoreactive T-cell responses, and confirmed the impaired uveitogenic capacity of T cells from these mice in an adoptive transfer experiment. Notably, one of these cross-reactive mAbs

---

Correspondence to, Feng Lin, Ph.D., Department of Immunology, Cleveland Clinic, Cleveland, OH 44195, linf2@ccf.org.

**Publisher's Disclaimer:** This is a PDF file of an unedited manuscript that has been accepted for publication. As a service to our customers we are providing this early version of the manuscript. The manuscript will undergo copyediting, typesetting, and review of the resulting proof before it is published in its final citable form. Please note that during the production process errors may be discovered which could affect the content, and all legal disclaimers that apply to the journal pertain.

The authors declare no conflict of financial interest.

significantly ameliorated retinal inflammation in EAU induced by the adoptive transfer of uveitogenic T cells.

**Conclusions**—Together, these data strongly suggest that CD6 plays a previously unknown, but pivotal role in autoimmune uveitis, and may be a promising new treatment target for this blinding disease. In addition, the newly developed mouse anti-mouse/human CD6 mAbs could be valuable tools for testing CD6-targeted therapies in other mouse models of human diseases.

## Introduction

Approximately 10% of all severe visual disabilities in the United States can be attributed to uveitic diseases. The most severe of these, autoimmune uveitis, which is commonly seen in certain rheumatic diseases including ankylosing spondylitis, juvenile rheumatoid arthritis and Behçet's disease, is characterized by T cell-mediated retinal destruction [1], and is estimated to affect more than 150,000 Americans annually [1]. Currently, the etiology of autoimmune uveitis remains unknown, and no cure has been identified. Much of our knowledge regarding the immunological mechanisms underlying human autoimmune uveitis was gleaned from studies of experimental autoimmune uveitis (EAU) [2], which is arguably the best currently available *in vivo* model for studying disease pathogenesis and developing novel therapies. EAU can be induced in C57BL/6 mice by immunization with interphotoreceptor retinoid-binding protein (IRBP) peptide 1-20 (IRBP<sub>1-20</sub>) or IRBP<sub>651-670</sub> [2-4], or in DBA-1 mice [5] by immunization with peptide IRBP<sub>161-180</sub> [2, 5]. EAU can also be induced by the adoptive transfer of activated IRBP-specific T cells into naïve mice [2]. Both human and animal studies of autoimmune uveitis have established that autoreactive T cells (Th1 and Th17 cells, with the latter playing the dominant role), rather than autoantibodies, are important for pathogenesis [6] [7] [8].

Although CD6 was among the first identified T cell antigens [9], its biological function remains elusive. The conflicting results of previous *in vitro* studies using different anti-CD6 monoclonal antibodies (mAbs) suggest that CD6 could either be a positive or negative regulator of T cell activation and function. Accordingly, the precise role of CD6 in autoimmune diseases remains poorly understood. No CD6-related clinical trials are currently ongoing in the US or Europe. However, itolizumab, an anti-human CD6 mAb developed in Cuba, was found to effectively reduce pathogenic T cell responses in patients with psoriasis and was recently approved for the treatment of that disease in India [10, 11]. When combined with methotrexate, itolizumab was also found to reduce T cell numbers and pro-inflammatory cytokine levels in patients with rheumatoid arthritis (RA) [12]. In addition, certain polymorphisms of the CD6 gene have been associated with increased risks of multiple sclerosis (MS) [13-16] and Behçet's disease [17], in which patients develop autoimmune uveitis.

The findings of previous clinical studies suggest that CD6 may be a valuable target for autoimmune disease treatment, but recent studies of collagen-induced arthritis (CIA), a model of RA, in CD6 knockout (KO) mice on the C57BL/6 background showed that the absence of CD6 led to exacerbated T cell responses to collagen and worsened joint inflammation [18]. However, our recent work involving experimental autoimmune

encephalomyelitis (EAE), a model of MS, in CD6 KO mice on the DBA/1 background demonstrated reduced autoreactive T cell responses and protection from central nervous system inflammation in these mice [19]. It remains unclear, however, whether these apparently conflicting results can be attributed to the different genetic backgrounds of the mice studied and/or to the differential roles of CD6 in various disease models.

In the present study, we immunized wild-type (WT) and CD6 KO mice (both on the DBA/1 background) with IRBP peptides to induce EAU, and compared disease severity using various ocular imaging techniques, including scanning laser ophthalmoscopy, spectral-domain optical coherence tomography, and visible light funduscopy. We also analyzed histopathological features and IRBP-specific T cell responses in these mice. To determine the feasibility of targeting CD6 for the treatment of EAU and autoimmune uveitis, we developed and characterized mouse anti-mouse CD6 mAbs with human CD6 cross-reactivity and tested the ability of one mAb to treat EAU induced by activated uveitogenic T cells.

## Methods

### Animals

WT DBA-1/J and C57BL/6J WT mice were obtained from The Jackson Laboratory (Bar Harbor, ME, USA). CD6 KO mice were generated on a DBA-1 background as previously described [19]. Sex- and age-matched (8–12 weeks) mice were used for all experiments. Mice were maintained under pathogen-free conditions in the animal facilities of the Lerner Research Institute, Cleveland Clinic. All animal care and experimental procedures were approved by the Institutional Animal Care and Use Committee of Cleveland Clinic and performed in accordance with the U.S. Department of Health and Human Services Guide for the Care and Use of Laboratory Animals.

### EAU induced by active immunization

Active immunization for EAU induction was performed as previously described [20]. In brief, an aqueous solution containing 200 µg IRBP<sub>161-180</sub> peptide (SGIPYHISYLHPGNTILHVD; custom synthesized by GenScript USA Inc., Piscataway, NJ, USA) was emulsified with an equal volume of complete Freund's adjuvant (CFA; Difco Laboratories, Inc., Detroit, MI, USA) containing 2.5 mg/ml *Mycobacterium tuberculosis* H37Ra (Difco Laboratories, Inc.) in a final volume of 200 µl. This emulsion was used to immunize DBA-1 WT and CD6 KO mice at the base of the tail (100 µl) and in each thigh (2 × 50 µl). Two hundred nanograms of pertussis toxin (List Biologic Laboratories, Inc., Campbell, CA, USA) were injected intraperitoneally immediately after immunization and on the following day.

### EAU induced by adoptive transfer of uveitogenic T cells

The adoptive transfer of uveitogenic T cells for EAU induction was performed according to a previously published protocol, with minor modifications [20]. First, each WT and CD6 KO mouse was immunized with 200 µg IRBP<sub>161-180</sub> peptide in CFA as described above. After 14 days, identical numbers of splenocytes from immunized WT and CD6 KO mice were

cultured in the presence of 10 µg/ml IRBP<sub>161-180</sub> peptide and 10 ng/ml IL-23 in RPMI 1640 with 10% fetal bovine serum (FBS) for 72 h. Activated (blasting) T cells were isolated by Ficoll centrifugation and 3×10<sup>6</sup> of the isolated T cells were injected intraperitoneally into each of the naïve WT recipient DBA/1J mice.

### Ocular fundus imaging and image analysis

For ocular imaging, topical endoscopy fundus imaging (TEFI), confocal scanning laser ophthalmoscopy (cSLO), and spectral-domain optical coherence tomography (SD-OCT) were performed as previously described [20]. Briefly, TEFI was performed to obtain a color fundus photo of the retina using a custom-fabricated apparatus containing a 3-mm pediatric endoscope and Nikon D90s digital SLR camera. cSLO (Heidelberg Retina Angiograph II; Heidelberg Engineering, Carlsbad, CA, USA) was performed to measure the infrared (IR) reflectance and autofluorescence (AF) at inner (e.g., vitreoretinal interface) and outer retinal locations (e.g., retinal pigmented epithelium-choroidal interface). AF was acquired at excitation and long-pass emission wavelengths of 488 nm and 500–680 nm, respectively. SD-OCT (840 HR SDOIS; Bioptigen, Inc., Morrisville, NC, USA) imaging was used to acquire detailed *in vivo* morphological information about the posterior pole, including the posterior lens, vitreous cavity, retina, and choroid. The imaging fields of view for cSLO and SD-OCT were 55° and 50°, respectively.

### Histopathological scoring

Whole eyes were collected, fixed in a 4% formaldehyde/phosphate-buffered saline (PBS) solution for 24 h, and embedded in paraffin. For histopathological analysis, 5-µm sections were cut through the pupil and optic nerve axis and stained with hematoxylin and eosin (H&E). The sections were assigned histopathological scores of 0–4 according to previously published criteria based on the inflammatory infiltration of and structural damage to the retina [2]. Score 0: No disease, normal retinal architecture. Score 0.5: Mild inflammatory cell infiltration of the retina with or without photoreceptor damage. Score 1: Mild inflammation and/or photoreceptor outer segment damage. Score 2: Mild to moderate inflammation and/or lesion extending to the outer nuclear layer. Score 3: Moderate to marked inflammation and/or lesion extending to the inner membrane layer. Score 4: Severe inflammation and/or full-thickness retinal damage.

### T cell recall assays

T cell recall assays were performed on day 21 after active immunization. Following erythrocyte lysis, 4×10<sup>5</sup> splenocytes per mouse were cultured without peptide, with 20 µg/mL of a non-relevant peptide (MOG 79–96), or with 20 µg/mL IRBP<sub>161-180</sub> peptide in 100 µl of RPMI 1640 medium supplemented with 10% FBS in a 96-well plate. After 72 h, the IFN-γ and IL-17A concentrations in the cell culture supernatants were determined using ELISA kits (BioLegend, San Diego, CA, USA).

### Development of mouse anti-mouse CD6 mAbs

CD6 KO mice were immunized subcutaneously with an emulsion containing 200 µg of recombinant mouse CD6 protein (R&D Systems, Minneapolis, MN, USA) and an equal

volume of CFA (1 mg/ml *M. tuberculosis* H37Ra). Two additional injections were administered at biweekly intervals starting 2 weeks after the initial immunization. Two weeks after the final boost, splenocytes from the immunized mice were fused with myeloma cells to develop hybridomas according to an established protocol [21].

### **Characterization of mouse anti-mouse CD6 mAbs and determination of human CD6 cross-reactivity**

A conventional ELISA was performed to screen antigen-specific mAbs in cell culture supernatants, using purified mouse or human CD6 protein (R&D Systems) as the target antigen. In brief, 2 µg/ml purified mouse or human CD6 protein was used to coat a plate at 4°C overnight. After blocking with 1% BSA in PBS for 1 h, the plate was incubated with cell culture supernatants at RT for 2 h. After washing, the plate was incubated with HRP-labeled anti-mouse IgG at RT for 1h, followed by color development by adding the HRP substrate TMB and OD<sub>450</sub> measurement using a microplate reader (Molecular Devices, San Jose, CA, USA). Clones with positive ELISA results were subsequently expanded, and the IgGs were purified and subjected to flow cytometric analyses of binding to CD6 on T cells from WT and CD6 KO mice and a human T cell line, Molt-4 [22].

### **Functional assay of mouse anti-mouse CD6 mAbs**

The ability to inhibit IFN $\gamma$  production from activated antigen-specific T cells was used as a measure of the T cell inhibitory activities of the identified mouse anti-mouse CD6 mAbs. Briefly, 4 $\times$ 10<sup>5</sup> splenocytes from ovalbumin (OVA)-specific TCR Tg (OT-II) mice were cultured in the presence or absence of 5 µg/ml OVA<sub>323–339</sub> peptide (InvivoGen, San Diego, CA, USA), as well as 10 µg/ml of the tested mAbs or control mouse IgG. Three days later, the IFN $\gamma$  concentrations in the supernatants were measured using an ELISA (BioLegend).

### **CD6-targeted treatment of EAU induced by the adoptive transfer of uveitogenic WT T cells**

C57BL/6J WT mice were actively immunized with 200 µg IRBP<sub>651–670</sub> peptide (LAQGAYRTAVDLESLASQLT; custom synthesized by GenScript USA Inc.) emulsified with CFA (2.5 mg/ml *M. tuberculosis* H37Ra), followed by a single intraperitoneal injection of 500 ng pertussis toxin. After 14 days, splenocytes from these mice were cultured for 72 h in the presence of 10 µg/ml IRBP peptide and 10 ng/ml IL-23 in RPMI 1640 with 10% FBS. Activated T cells were isolated by Ficoll centrifugation, after which 5 $\times$ 10<sup>6</sup> cells were administered intraperitoneally to each naive WT recipient mouse [20]. These adoptively transferred mice were randomly divided into two groups: one group was injected intraperitoneally with 200 µg of the 6C1 mAb on days 0, 4, and 7 post-transfer, whereas the other group received the same amount of mouse IgG at the same time points.

### **Immunohistochemical staining of T cell infiltrates**

Mouse eyes were collected and fixed in 4% PFA, embedded in paraffin, and cut into 5-µm sections through the pupil–optic nerve axis. Subsequently, the sections were deparaffinized, unmasked, and rehydrated prior to staining using a polyclonal rabbit anti-CD3 (Abcam, Cambridge, MA, USA) as the primary Ab, followed by staining with a goat anti-rabbit AP-polymer (Biocare Medical, Pacheco, CA, USA) as the secondary Ab. Sections stained

without the primary antibody were included as controls. The reactions were visualized using the Vulcan Fast Red Chromogen Kit 2 (Biocare Medical), and hematoxylin was used as the counterstain.

### Statistical analysis

GraphPad Prism 6 (GraphPad Software, Inc., La Jolla, CA, USA) was used for data analysis. Data are expressed as means  $\pm$  standard deviations (SD). All data sets were tested for the normal distribution. Mann-Whitney test, Student's t-test or a one-way analysis of variance (ANOVA) were selected respectively, according to the normality and the number of data sets. The EAU clinical scores were analyzed using a two-way (ANOVA). P values of  $<0.05$  were considered significant.

## Results

### CD6 KO mice are protected from retinal injury after EAU induction

Although certain CD6 polymorphisms have been associated with Behçet's disease [17], the potential role of CD6 in the pathogenesis of autoimmune uveitis, positive or negative, remains unknown. To address this issue, we compared the induction of EAU in age- and sex-matched CD6 KO (n=18) and WT mice (n=17) on a DBA/1 background following immunization with peptide IRBP<sub>161-180</sub> in CFA and pertussis toxin according to a published protocol [5].

We first examined eyes harvested from randomly selected WT and CD6 KO mice 14 days after immunization, using various *in vivo* ocular imaging techniques commonly used for evaluation of uveitis severity in patients. On average, we found that WT mice developed more severe uveitis after EAU induction, compared to CD6 KO mice. Figure 1 shows representative fundus images obtained using TEFI and cSLO. The TEFI comparison (Fig. 1 A, B) revealed a lack of contrast in the WT eye relative to the CD6 KO eye, as demonstrated by the ability (CD6 KO) or inability (WT) to visualize the choroidal vasculature and optic disk. The hazy appearance in the WT eye (Fig. 1A, arrow) can be attributed to inflammation near the optic nerve, which is absent in CD6 KO mice. Occasionally, dark spots that were identified as cell aggregations on the posterior or anterior lens surface or surface-adherent iris fragments were observed in the eyes of WT mice (Fig. 1A, star).

We used cSLO (Fig. 1C–J) to further dissect the posterior pole inflammatory responses observed by TEFI. In the inner retina, IR-cSLO images specifically trained on the vitreoretinal interface (VRI) revealed changes in the appearance (e.g., caliber) and reflectivity of the retinal vasculature and nerve fibers, respectively (Fig. 1C, D). Although AF-cSLO of the VRI indicated AF foci (AFF) indicative of inflammatory cells in both groups, more of these foci were observed in WT mice relative to CD6 KO mice (Fig. 1E, F). In the outer retina, more elongated hyper-reflective nodes were observed around the optic disk in the region nearest the RPE-choroid complex in WT mice, compared to CD6 KO mice (Fig. 1G–J). This finding was most often observed in animals with more severe posterior ocular inflammation, as observed using the trifecta of imaging techniques.



The representative SD-OCT B-scan images of the posterior pole in Figure 2 revealed inflammation-induced pathology relative to in-depth tissue morphology. Hyper-reflective nodes located on opposite sides of the optic nerve and within the outer retina can be observed in both WT and CD6 KO mice (Fig. 1K, M). Hyper-reflective foci in the vitreous cavity are suggestive of infiltrating cells and/or cellular aggregates. After applying a threshold to better accentuate these foci (Fig. 1L, N), we found that both the total particle count (WT,  $113.90 \pm 66.82$  vs. CD6 KO,  $44.38 \pm 26.27$ ,  $p=0.003$ ; Fig. 1O) and particle size (WT,  $566.00 \pm 228.66$  vs. CD6 KO,  $292.80 \pm 208.35$ ,  $p=0.038$ ; Fig. 1P) in the vitreous cavities were significantly larger in the WT mice than in the CD6 KO mice.

After 21 days, we euthanized the mice and harvested the eyes. The severity of retinal inflammation was assessed by H&E staining, followed by a histopathological analysis to assign severity scores. Consistent with the results from live fundus imaging assays, the eyes of WT mice exhibited prominent outer retinal folds, undulations, and hypertrophy that occasionally protruded into the inner retina (Fig. 2A). Compared to the mean histopathological score of  $0.625 \pm 0.62$  in WT mice subjected to EAU, similarly treated CD6 KO mice exhibited significantly less retinal inflammation, with a mean score of  $0.125 \pm 0.18$  ( $p=0.003$ ; Fig. 2B). All ocular imaging findings and histopathological analyses clearly demonstrated that CD6 KO mice were protected from retinal injury in EAU.

### CD6 KO mice exhibit reduced IRBP-specific T cell responses after EAU induction

In addition to the above comparison of retinal inflammation severity between WT and CD6 KO mice after EAU induction, we also compared IRBP<sub>161-180</sub>-specific Th1 and Th17 responses in these mice by measuring the production of IFN $\gamma$  (Fig. 2C) and IL-17 (Fig. 2D) from splenocytes collected 21 days after immunization. Through *ex vivo* recall assays, we demonstrated that after re-stimulation, IRBP-specific splenic T cells from WT and CD6 KO mice with EAU produced  $21.82 \pm 10.41$  v.s.  $4.85 \pm 0.58$  ng/ml of IFN $\gamma$ , respectively, and  $11.40 \pm 6.50$  v.s.  $2.63 \pm 1.35$  ng/ml of IL-17, respectively. In summary, CD6 KO mice with EAU exhibited markedly decreased IRBP-specific Th1 and Th17 responses. These cytokine findings, which were consistent with the significantly reduced retinal inflammation observed using histopathological analyses and various ocular imaging techniques, suggest that CD6 is required for the development of pathogenic T cell responses in EAU.

### Adoptive transfer of CD6 KO IRBP-specific T cells induces attenuated EAU in naïve WT mice

To demonstrate that CD6 deficiency impairs the induction of uveitogenic T cells, we performed T cell adoptive transfer of donor cells from WT and CD6 mice immunized with IRBP<sub>161-180</sub> peptide in CFA, as described for the active immunization-induced EAU experiments. After 14 days, we incubated splenocytes from immunized WT and CD6 KO mice in the presence of the same IRBP peptide plus IL-23. After 3 days, we enriched the activated (blasting) T cells and administered the same number of them into each of the naïve WT DBA/1 mice as described in the Methods. We then used indirect funduscopy to monitor EAU development and recorded the clinical scores daily for 14 days. After the adoptive transfer, naïve WT mice that had received WT uveitogenic T cells developed significantly more severe EAU, compared to mice that had received CD6 KO uveitogenic T cells (Fig.

3A). These data, together with the finding described above, that CD6 KO mice developed significantly less severe retinal inflammation during active immunization-induced EAU, strongly suggest that CD6 could be a target for the treatment of EAU.

### **Development of mouse anti-mouse CD6 mAbs**

The successful treatment of EAU with anti-CD6 mAbs would validate CD6 as a therapeutic target in autoimmune uveitis. However, all the currently available anti-mouse CD6 mAbs were developed in rats. As rat IgGs are highly immunogenic in mice, we observed that mice treated with a rat anti-mouse CD6 mAb rapidly developed high titers of anti-rat IgG antibodies (data not shown). To overcome this issue in future treatment studies in mice, we developed function-neutralizing mouse anti-mouse CD6 mAbs using CD6 KO mice. In brief, we immunized CD6 KO mice with recombinant mouse CD6 protein and subsequently generated hybridomas following standard protocols. We used ELISA to identify 28 positive hybridoma clones, and screened all positive clones via flow cytometry using WT and CD6 KO T cells to determine the abilities of these mAbs to bind the extracellular regions of mouse CD6 under physiological conditions. Finally, we identified seven clones that labeled WT but not CD6 KO T cells (data not shown).

### **Identification of functional mouse anti-mouse CD6 antibodies**

To select function-blocking mouse anti-mouse CD6 IgGs, we purified IgGs from five of the seven clones identified in the above-described flow cytometry assay and tested these in an *in vitro* CD6 function-blocking assay to determine their abilities to inhibit IFN $\gamma$  production from activated antigen-specific T cells. In brief, we first cultured splenocytes from OT-II mice in the presence of OVA and each individual purified mAb (clone 2H10, 3C12, 4B8, 4F8, or 6C1) or the same concentration of control mouse IgG, as described above. Next, we compared the abilities of these mAbs to inhibit cytokine production from OVA-specific T cells by measuring the levels of IFN $\gamma$  in the culture supernatants. Of the tested clones, 4B8, 4F8, and 6C1 inhibited antigen-specific T cell activity (Fig. 3B).

### **Identification of mouse anti-mouse CD6 mAbs with human CD6 cross-reactivity**

Mouse CD6 shares approximately 80% homology with human CD6. Therefore, we also screened the identified mouse anti-mouse CD6 mAbs for cross-reactivity with human CD6 in a flow cytometry assay with the human T cell line, Molt-4 [23]. Whereas clones 2H10, 3C12, and 4F8 were specific for mouse CD6 (Fig. 3C), clones 6C1 and 4B8 cross-reacted with human CD6 (Fig. 3D). This highly interesting finding suggests that these mAbs, if proven to effectively treat EAU in mice, could be directly humanized in the context of a new therapy for uveitis in humans.

### **The mouse anti-mouse CD6 mAb effectively treats EAU induced by already activated uveitogenic T cells**

Uveitis patients with clinical disease already harbor activated uveitogenic T cells. Therefore, EAU induced by the adoptive transfer of pre-activated uveitogenic T cells would provide a good model in which to test potentially clinically relevant treatment reagents. Using an established protocol, we again induced EAU in naïve WT C57BL/6 mice by adoptively



transferring uveitogenic IRBP<sub>651-670</sub>-specific T cells prepared *in vitro*. Subsequently, half of the recipients were randomly selected and treated with a mouse anti-mouse CD6 mAb exhibiting cross-reactivity with human CD6 (clone 6C1) or the same amount of mouse IgG. We followed the development of EAU in these mice by indirect ophthalmoscopy and assigned EAU clinical scores each day. We additionally evaluated the severity of uveitis on day 14 using TEFI, cSLO and SD-OCT.

Compared to mice treated with mouse IgG (controls), which developed severe EAU (clinical scores up to 2.5), mice treated with the 6C1 mAb clone developed very mild retinal inflammation (approximate clinical scores of 0.5; Fig. 4A). TEFI imaging also identified numerous affected regions in control mice that were also observed in IR- and AF-cSLO analyses of the RPE-choroid complex in the outer retina (Fig. 4B, C). Specifically, IR-cSLO (Fig. 4D–K) showed a hyper-reflective outer retinal region that matched a region observed in the TEFI image, while AF-cSLO indicated retinal folds similar to, but more pronounced than, those previously observed in WT DBA-1 mice. In the inner retina, AF-cSLO revealed many AFF at the VRI, some of which were adjacent to retinal vessels. The folds and undulations, which were more clearly observed at the outer retinal focus position, had caused increases in the background of the inner retina at the VRI AF-cSLO focus position. By contrast, these imaging findings were overwhelmingly absent in anti-CD6 mAb-treated mice, as demonstrated by the quantitative SD-OCT results (Fig. 5). Specifically, both the total particle count (control,  $185.30 \pm 88.35$  vs. treated,  $19.69 \pm 8.38$ ,  $p=0.0286$ ; Fig. 5E) and particle size (control,  $3049.00 \pm 1025.68$  vs. treated,  $198.60 \pm 86.80$ ,  $p=0.0286$ ; Fig. 5F) differed significantly between control and mouse anti-mouse CD6 IgG-treated EAU mice.

In addition to the above-described live-imaging analyses, we euthanized the mice 18 days after EAU induction and subjected the eyes to histopathological scoring and immunohistochemical staining to quantitate the numbers of ocular-infiltrating T cells. Notably, anti-CD6 mAb-treated mice had significantly lower histopathological scores than did control mice ( $0.14 \pm 0.19$  vs.  $0.89 \pm 0.45$ ,  $p=0.002$ ; Fig. 6A, B). Additionally, the eyes of control mice contained a mean of  $35.63 \pm 20.89$  infiltrating CD3<sup>+</sup> T cells, compared to only  $7.625 \pm 11.34$  CD3<sup>+</sup> T cells in the anti-CD6 mAb-treated mice,  $p=0.003$  (Fig. 6C, D). Taken together, these findings demonstrate that our developed mouse anti-mouse CD6 mAb (clone 6C1) could effectively treat EAU induced by already-activated uveitogenic T cells.

## Discussion

In this work, we observed significantly reduced retinal inflammation, as well as impaired antigen-specific Th1/Th17 responses, in CD6 KO mice following active immunization to induce EAU. Our findings suggest a pivotal role for CD6 both in the development of EAU and as an effective target in the treatment of this disease. Indeed, we additionally developed and identified mouse anti-mouse CD6 mAbs that cross-react with human CD6 by immunizing CD6 KO mice with recombinant mouse CD6 protein. At least one of these mAbs could effectively treat EAU induced by the adoptive transfer of pre-activated uveitogenic T cells, which further supports the concept of CD6 as a novel and valid target for the treatment of autoimmune uveitis.

Although CD6 has long been speculated a potential therapeutic target in autoimmune diseases, previous *in vitro* studies have yielded conflicting results, and CD6 gene-engineered animals for *in vivo* studies were previously unavailable. As noted earlier, however, the observed effectiveness of the humanized anti-CD6 mAb itolizumab led to its approval for the treatment of psoriasis in India [24]. Furthermore, itolizumab was found to induce fewer side effects (e.g., opportunistic infections) in patients with psoriasis, compared to many other similar biologicals such as infliximab, an anti-TNF $\alpha$  mAb [11, 25, 26]. Itolizumab was also found to attenuate joint inflammation in patients with RA when used together with methotrexate in a clinical trial [12, 27]. In addition to these positive clinical results, which strongly support the validity of CD6 as target for autoimmune disease treatment, several groups have recently identified the CD6 gene as associated with the risk of MS through genome-wide association studies [13-16]. It is perhaps notable in this context that MS can also be associated with uveitis. Optic neuritis is often the first manifestation of MS, and a proportion of MS patients have an associated uveitis [28, 29]. Furthermore, in another genetic study directly related to this report, certain CD6 gene polymorphisms associated with MS have also been associated with Behçet's disease [17], a condition in which patients develop autoimmune uveitis, thus suggesting that CD6 plays an important role in the pathogenesis of autoimmune uveitis.

In contrast to clinical and genetic studies suggesting that a lack of CD6 function would reduce T cell responses *in vivo* and ameliorate autoimmune disease severity, a recent study found that CD6 KO mice on a C57BL/6 background developed augmented autoreactive T cell responses and exacerbated joint inflammation associated with collagen-induced arthritis [18]. These results differ from our study of EAE in CD6 KO mice on a DBA/1 background [19], in which we found that CD6-deficient T cells similarly exhibited augmented activation but also suffered impaired proliferation and survival, leading to an overall dampening of autoreactive T cell responses and amelioration of central nervous system inflammation after immunization with the MOG peptide. In addition, compared to WT T cells, CD6 KO T cells exhibited a deficient ability to migrate through a brain microvascular endothelial cell monolayer [19], suggesting that CD6 is also important for T cell migration through the blood-brain barrier during EAE development. Because EAU and EAE are pathogenically very similar, we believe that the mechanisms discovered in studies of EAE in CD6 KO mice [19] would also apply to the studies of EAU described herein.

In our recently published work [19], we also demonstrated that treatment with a mouse-anti-human CD6 mAb could very effectively reduce pathogenic T cell responses in CD6 humanized mice and attenuate the severity of EAE without T cell depletion. The results from our present study of EAU in CD6 KO mice, as well as the successful development and application of mouse anti-mouse CD6 mAbs for the treatment of EAU, confirm the CD6 KO mouse phenotype discovered in our previous EAE studies and suggest that the previously identified pathogenic role of CD6 is not unique to EAE. These new EAU-related data, together with data from related clinical studies, enforce the idea that CD6 could be targeted to treat these autoimmune diseases. The apparent differences between genetically distinct mouse strains (C57BL/6 vs. DBA/1) in terms of the role of CD6 in autoimmune disease development suggests a potentially heterogeneous role of CD6 in various human autoimmune conditions. However, additional studies are required to validate this hypothesis.

Most available mAbs against mouse antigens were generated in rats and hamsters, and many pre-clinical treatment studies involved the direct injection of these rat or hamster IgGs into mice for efficacy evaluations. However, these foreign IgGs are highly immunogenic and elicit the production of anti-mAb antibodies in mice, resulting in impaired function or even false negative results. Similarly, we found that mice injected with a rat anti-mouse CD6 IgG rapidly produced high titers of anti-rat IgG antibodies (data not shown). Accordingly, we developed mouse anti-mouse CD6 mAbs to minimize these complications in long-term and repetitive treatment studies. To avoid immune tolerance issues during hybridoma development, we immunized CD6 KO mice, which never “see” CD6; accordingly, immunization with recombinant mouse CD6 protein provoked strong and specific immune responses in these mice and yielded many good anti-CD6 hybridoma clones. Using ELISA and flow cytometric analyses, we first identified mouse anti-mouse CD6 mAbs reactive to surface CD6 epitopes, and subsequently selected functional mAbs using the T cell inhibitory assay. Additionally, the high homology between mouse and human CD6 allowed us to identify several functional mouse anti-mouse CD6 mAbs with cross-reactivity to human CD6. These latter mAbs will be clinically valuable in the future, not only because they are non-immunogenic in mice and can therefore be administered repetitively and over long periods during proof-of-concept studies, but also because they are cross-reactive to human CD6 and can therefore be directly humanized for further clinical development.

In summary, we found reduced autoreactive T cell responses and significantly attenuated retinal inflammation in a CD6 KO mouse model of EAU. Additionally, we developed functional mouse anti-mouse CD6 mAbs with cross-reactivity to human CD6 and demonstrated the efficacy of one of these mAbs in the treatment of EAU induced by pre-activated uveitogenic T cells. These findings demonstrate a previously unknown but pivotal role of CD6 in the pathogenesis of EAU and suggest that anti-CD6 mAbs could be developed as novel therapeutic agents for autoimmune uveitis, a leading cause of blindness for which a cure remains elusive.

## Supplementary Material

Refer to Web version on PubMed Central for supplementary material.

## Acknowledgments

This work was supported in part by NIH grants EY025373, EY025585 and EY11373.

## References

1. Gritz DC, Wong IG. Incidence and prevalence of uveitis in Northern California; the Northern California Epidemiology of Uveitis Study. *Ophthalmology*. 2004; 111:491–500. discussion. [PubMed: 15019324]
2. Caspi RR. Experimental autoimmune uveoretinitis in the rat and mouse. *Curr Protoc Immunol*. 2003 Chapter 15: Unit 15 6.
3. Mattapallil MJ, Silver PB, Cortes LM, St Leger AJ, Jittayasothorn Y, Kielczewski JL, et al. Characterization of a New Epitope of IRBP That Induces Moderate to Severe Uveoretinitis in Mice With H-2b Haplotype. *Invest Ophthalmol Vis Sci*. 2015; 56:5439–49. [PubMed: 26284549]

4. Zhang L, Bell BA, Yu M, Chan CC, Peachey NS, Fung J, et al. Complement anaphylatoxin receptors C3aR and C5aR are required in the pathogenesis of experimental autoimmune uveitis. *Journal of leukocyte biology*. 2015
5. Jiang HR, Wei X, Niedbala W, Lumsden L, Liew FY, Forrester JV. IL-18 not required for IRBP peptide-induced EAU: studies in gene-deficient mice. *Investigative ophthalmology & visual science*. 2001; 42:177–82. [PubMed: 11133864]
6. Caspi RR. Th1 and Th2 responses in pathogenesis and regulation of experimental autoimmune uveoretinitis. *Int Rev Immunol*. 2002; 21:197–208. [PubMed: 12424843]
7. Amadi-Obi A, Yu CR, Liu X, Mahdi RM, Clarke GL, Nussenblatt RB, et al. TH17 cells contribute to uveitis and scleritis and are expanded by IL-2 and inhibited by IL-27/STAT1. *Nature medicine*. 2007; 13:711–8.
8. Luger D, Silver PB, Tang J, Cua D, Chen Z, Iwakura Y, et al. Either a Th17 or a Th1 effector response can drive autoimmunity: conditions of disease induction affect dominant effector category. *J Exp Med*. 2008; 205:799–810. [PubMed: 18391061]
9. Kamoun M, Kadin ME, Martin PJ, Nettleton J, Hansen JA. A novel human T cell antigen preferentially expressed on mature T cells and shared by both well and poorly differentiated B cell leukemias and lymphomas. *J Immunol*. 1981; 127:987–91. [PubMed: 6790625]
10. Krupashankar DS, Dogra S, Kura M, Saraswat A, Budamakuntla L, Sumathy TK, et al. Efficacy and safety of itolizumab, a novel anti-CD6 monoclonal antibody, in patients with moderate to severe chronic plaque psoriasis: Results of a double-blind, randomized, placebo-controlled, phase-III study. *Journal of the American Academy of Dermatology*. 2014
11. Menon R, David BG. Itolizumab - a humanized anti-CD6 monoclonal antibody with a better side effects profile for the treatment of psoriasis. *Clin Cosmet Investig Dermatol*. 2015; 8:215–22.
12. Aira LE, Hernandez P, Prada D, Chico A, Gomez JA, Gonzalez Z, et al. Immunological evaluation of rheumatoid arthritis patients treated with itolizumab. *MAbs*. 2016; 8:187–95. [PubMed: 26466969]
13. International Multiple Sclerosis Genetics C. The genetic association of variants in CD6, TNFRSF1A and IRF8 to multiple sclerosis: a multicenter case-control study. *PLoS One*. 2011; 6:e18813. [PubMed: 21552549]
14. Swaminathan B, Matesanz F, Cavanillas ML, Alloza I, Otaegui D, Olascoaga J, et al. Validation of the CD6 and TNFRSF1A loci as risk factors for multiple sclerosis in Spain. *J Neuroimmunol*. 2010; 223:100–3. [PubMed: 20430450]
15. De Jager PL, Jia X, Wang J, de Bakker PI, Ottoboni L, Aggarwal NT, et al. Meta-analysis of genome scans and replication identify CD6, IRF8 and TNFRSF1A as new multiple sclerosis susceptibility loci. *Nat Genet*. 2009; 41:776–82. [PubMed: 19525953]
16. Heap GA, Yang JH, Downes K, Healy BC, Hunt KA, Bockett N, et al. Genome-wide analysis of allelic expression imbalance in human primary cells by high-throughput transcriptome resequencing. *Hum Mol Genet*. 2010; 19:122–34. [PubMed: 19825846]
17. Zheng M, Zhang L, Yu H, Hu J, Cao Q, Huang G, et al. Genetic polymorphisms of cell adhesion molecules in Behcet's disease in a Chinese Han population. *Sci Rep*. 2016; 6:24974. [PubMed: 27108704]
18. Orta-Mascardo M, Consuegra-Fernandez M, Carreras E, Roncagalli R, Carreras-Sureda A, Alvarez P, et al. CD6 modulates thymocyte selection and peripheral T cell homeostasis. *J Exp Med*. 2016; 213:1387–97. [PubMed: 27377588]
19. Li Y, Singer NG, Whitbred J, Bowen MA, Fox DA, Lin F. CD6 as a potential target for treating multiple sclerosis. *Proc Natl Acad Sci U S A*. 2017; 114:2687–92. [PubMed: 28209777]
20. Zhang L, Bell BA, Yu M, Chan CC, Peachey NS, Fung J, et al. Complement anaphylatoxin receptors C3aR and C5aR are required in the pathogenesis of experimental autoimmune uveitis. *J Leukoc Biol*. 2016; 99:447–54. [PubMed: 26394814]
21. Wood JN. Immunization and fusion protocols for hybridoma production. *Methods Mol Biol*. 1984; 1:261–70. [PubMed: 20512695]
22. Mertelsmann R, Gillis S, Steinmann G, Ralph P, Stiehm M, Koziner B, et al. T-cell growth factor (interleukin 2) and terminal transferase activity in human leukemias and lymphoblastic cell lines. *Blut*. 1981; 43:99–103. [PubMed: 6942897]

23. Minowada J, Onuma T, Moore GE. Rosette-forming human lymphoid cell lines. I. Establishment and evidence for origin of thymus-derived lymphocytes. *J Natl Cancer Inst.* 1972; 49:891–5. [PubMed: 4567231]
24. Jayaraman K. Biocon's first-in-class anti-CD6 mAb reaches the market. *Nature biotechnology.* 2013; 31:1062–3.
25. Dogra S, Uprety S, Suresh SH. Itolizumab, a novel anti-CD6 monoclonal antibody: a safe and efficacious biologic agent for management of psoriasis. *Expert Opin Biol Ther.* 2017; 17:395–402. [PubMed: 28064543]
26. Parthasaradhi A. Safety and Efficacy of Itolizumab in the Treatment of Psoriasis: A Case Series of 20 Patients. *J Clin Diagn Res.* 2016; 10:WD01–WD3.
27. Chopra A, Chandrashekara S, Iyer R, Rajasekhar L, Shetty N, Veeravalli SM, et al. Itolizumab in combination with methotrexate modulates active rheumatoid arthritis: safety and efficacy from a phase 2, randomized, open-label, parallel-group, dose-ranging study. *Clin Rheumatol.* 2016; 35:1059–64. [PubMed: 26050104]
28. Kaya D, Kaya M, Ozakbas S, Idiman E. Uveitis associated with multiple sclerosis: complications and visual prognosis. *Int J Ophthalmol.* 2014; 7:1010–3. [PubMed: 25540756]
29. Cunningham ET Jr, Pavesio CE, Goldstein DA, Forooghian F, Zierhut M. Multiple Sclerosis-Associated Uveitis. *Ocul Immunol Inflamm.* 2017; 25:299–301. [PubMed: 28696171]

**Highlights**

- CD6 is required for the development of experimental autoimmune uveitis (EAU)
- CD6 KO mice developed attenuated autoreactive T cell responses in EAU
- Uveitogenic T cells from CD6 KO mice have impaired capacity in inducing EAU
- Mouse anti-mouse CD6 monoclonal antibodies (mAbs) are generated using the CD6 KO mice
- Treating mice adoptively transferred with uveitogenic T cells with one of the mouse anti-mouse CD6 mAbs is effective in reducing retinal inflammation



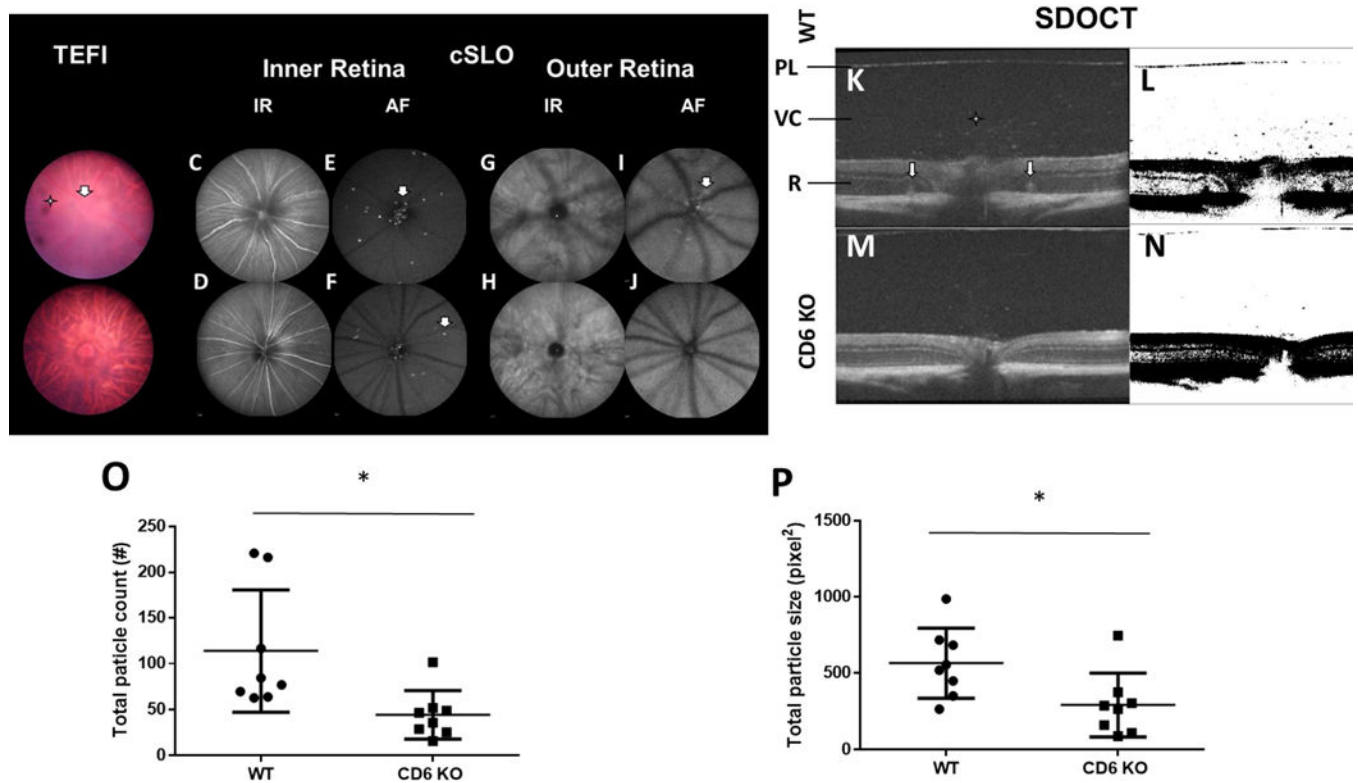


**Figure 1.** Representative images from topical endoscopy fundus imaging (TEFI), confocal scanning laser ophthalmoscopy (cSLO) analyses, spectral-domain optical coherence tomography (SD-OCT) imaging and analyses of wild-type (WT) and CD6 knockout (KO) mice on a DBA-1 background on day 14 after the induction of experimental autoimmune uveitis (EAU). A and B: TEFI revealed less severe EAU in CD6 KO mice than in WT mice. The hazy area (arrow) in the WT mouse fundus was caused by cellular infiltration of the vitreous chamber, as well as a retinal lesion and edema. The dark spots (star) were identified as cell aggregations or iris fragments adherent to the lens surface. TEFI of CD6 KO mice showed clear choroidal vessels through the retina. C–F: cSLO images of the inner layer of the retina revealed more hyper-reflective features in WT mice, compared to CD6 KO mice. In the former, more numerous foci (arrows) suggestive of infiltrating cells were observed around the optical nerve and adjacent to the retinal vessels. G–J: In the outer layer of the retina, hyper-reflective nodes (arrow) indicative of retinal edema or folds encircled the optical nerve in WT mice. K and M: SD-OCT images revealed more reflective foci (star) and retinal folds (arrows) in WT mice relative to CD6 KO mice. PL: posterior lens margin, VC: vitreous cavity, R: retina. L and N: Analysis of vitreous particles on SD-OCT images processed using ImageJ. O and P: Reductions in the total particle count and size were observed in the vitreous cavities of CD6 KO mice relative to WT mice. Each dot represents one mouse. Data are shown as means  $\pm$  standard deviations. N=8 per group. \* $p < 0.05$ , Mann-Whitney test.

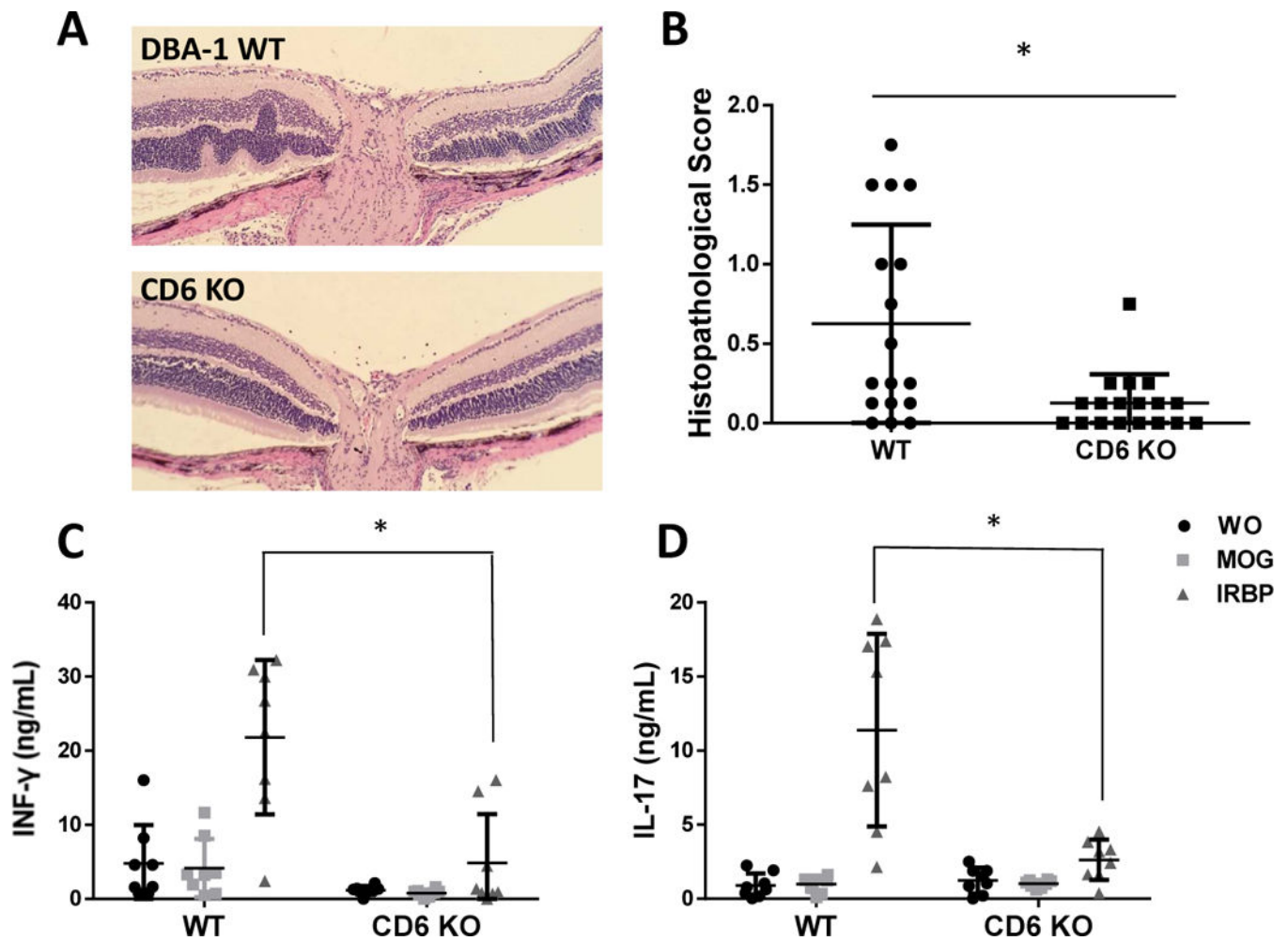


**Figure 2.** Histopathological and immunological analyses of wild-type (WT) and CD6 knockout (KO) mice with experimental autoimmune uveitis (EAU). A and B: Representative histopathological images and scores for WT and CD6 KO on day 21 after immunization to induce EAU. The WT samples exhibited prominent retinal folds and occasional protrusions, whereas CD6 KO mice exhibited significantly fewer histopathological changes and lower scores. Data are shown as means  $\pm$  standard deviations (SD). N=17 and 18 in the WT and CD6 KO groups, respectively. \*  $p < 0.05$ , Student's t-test. C and D: CD6 KO mice exhibited decreased IRBP-specific T cell responses after immunization. Data are shown as means  $\pm$  SD. N=8, one-way ANOVA.

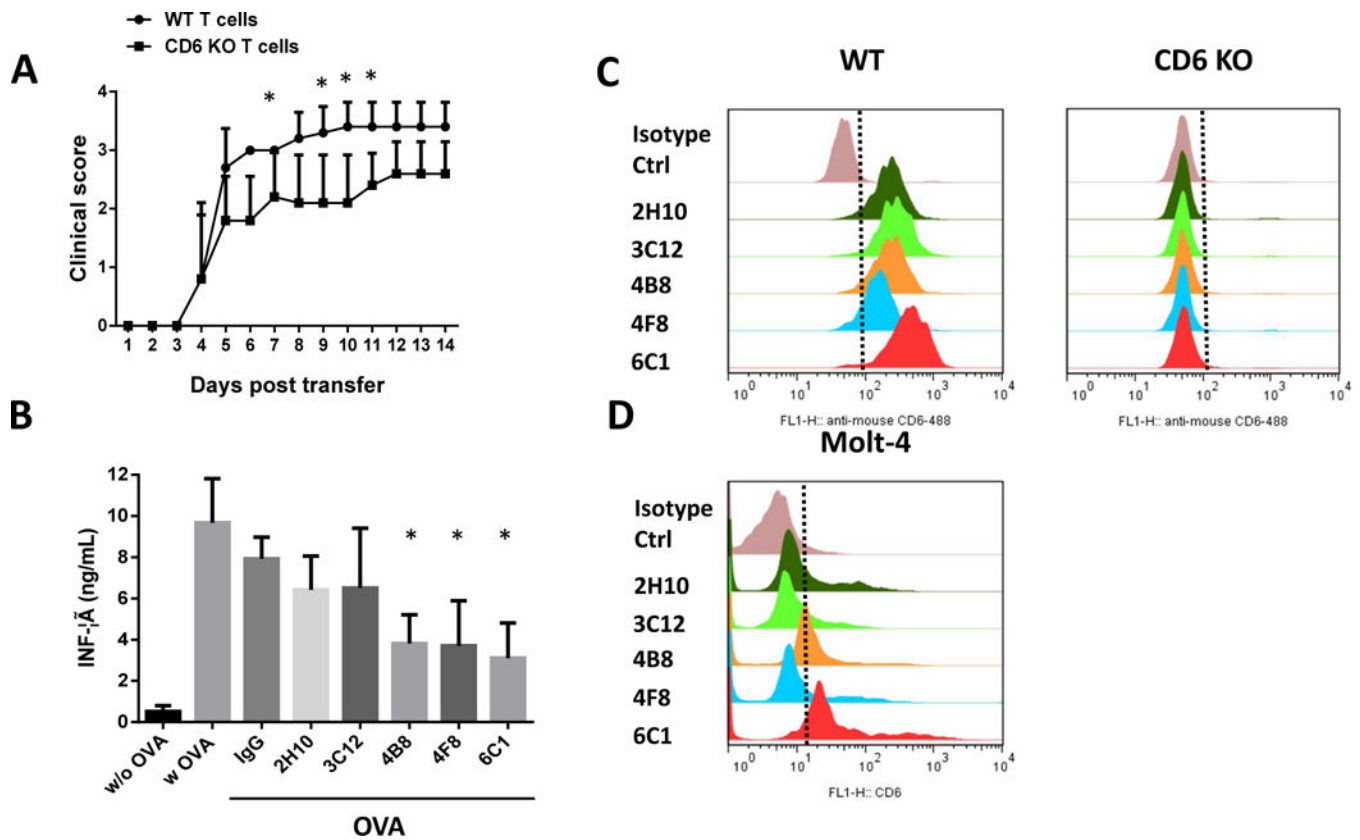


**Figure 3.**

A: CD6 knockout (KO) T cells have an impaired capacity to induce experimental autoimmune uveitis (EAU). Uveitogenic T cells from wild-type (WT) and CD6 KO mice were amplified *in vitro* and adoptively transferred into naïve WT DBA/1 mice to induce EAU. Mice that received WT uveitogenic T cells developed more severe disease than did those that received CD6 KO uveitogenic T cells. Data are shown as means  $\pm$  standard deviations. N=5 per group. \* $p$  < 0.05, two-way ANOVA. B–D: Development of functional mouse anti-mouse CD6 antibodies with human CD6 cross-reactivity. B: Different clones of the resultant mouse anti-mouse CD6 mAbs were tested in a CD6 function blocking assay *in vitro*. Of the five clones tested, three (4B8, 4F8, and 6C1) inhibited IFN- $\gamma$  production from activated antigen-specific T cells. Data are shown as means  $\pm$  standard deviations. One-way ANOVA. C: A flow cytometry analysis using wild-type and CD6 KO mouse T cells showed that all five purified IgGs selectively bound to mouse CD6. D: A flow cytometry analysis using the human T cell line Molt-4 revealed that clones 4B8 and 6C1 cross-reacted with human CD6.

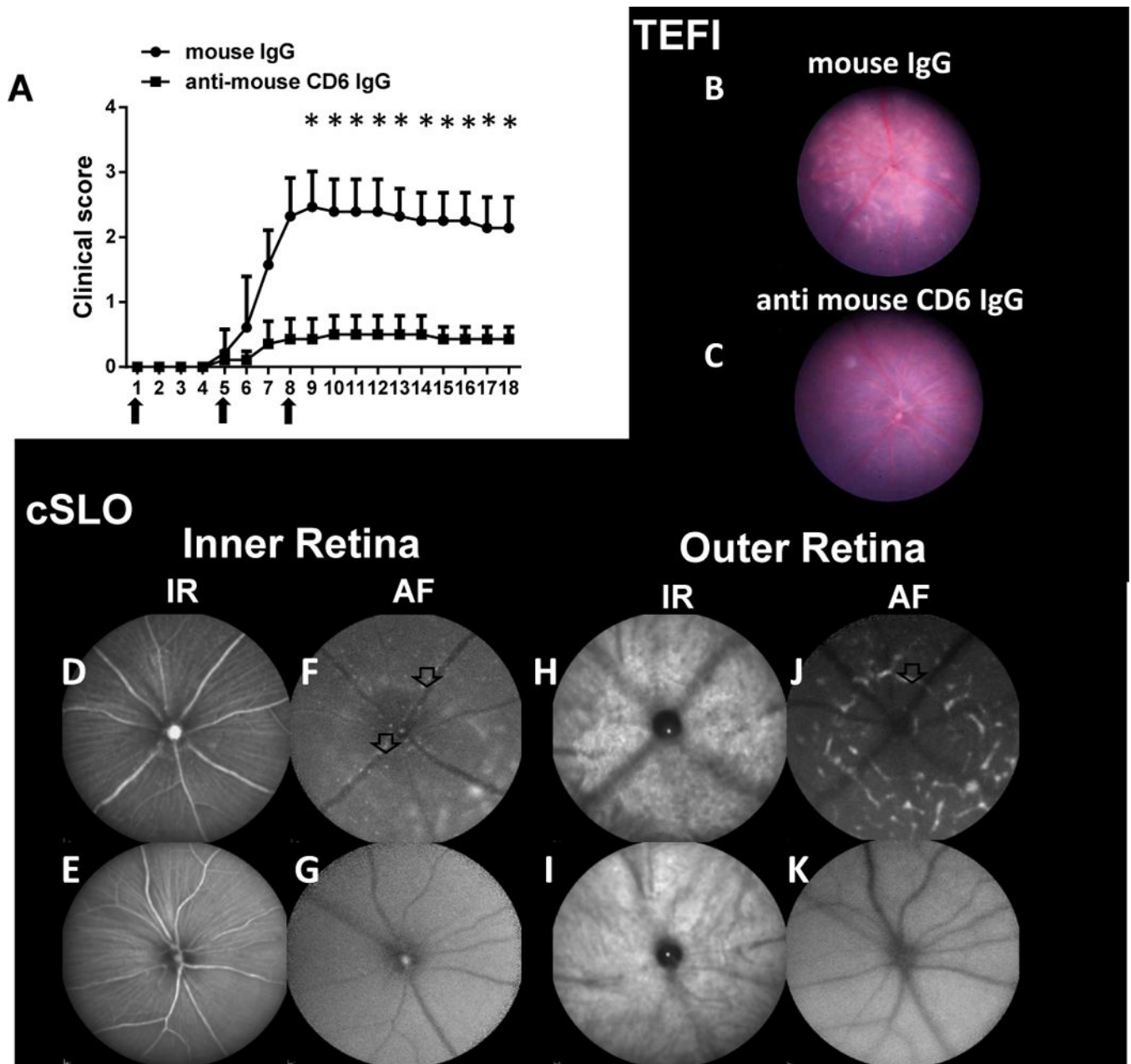


**Figure 4.**

Treatment studies using a newly developed mouse anti-mouse CD6 mAb. **A:** Mice with experimental autoimmune uveitis (EAU) induced by the adoptive transfer of uveitogenic T cells exhibited reduced clinical scores when treated with the mouse anti-mouse CD6 mAb clone 6C1. Briefly, 200  $\mu$ g of 6C1 or mouse IgG were administered on days 0, 4 and 7 (arrows). Data are shown as means  $\pm$  standard deviations.  $N=7$  per group. \*  $p < 0.05$ , two-way ANOVA. **B–K:** Representative images from topical endoscopy fundus imaging (TEFI) and confocal scanning laser ophthalmoscopy (cSLO) of control and CD6 mAb-treated mice on Day 8 after adoptive transfer. **B** and **C:** TEFI images revealed reduced retinal damage caused by uveitogenic T cells after treatment with the anti-mouse CD6 IgG. Multiple retinal

lesions (arrow) were observed in mice treated with IgG (control), whereas many fewer lesions were observed in CD6 mAb-treated mice. D–K: Hyper-reflective foci (arrows) and large retinal lesions (marked area) were observed in cSLO images from the control group, but were rarely observed in images from the CD6 mAb-treated group.

Author Manuscript

Author Manuscript

Author Manuscript

Author Manuscript

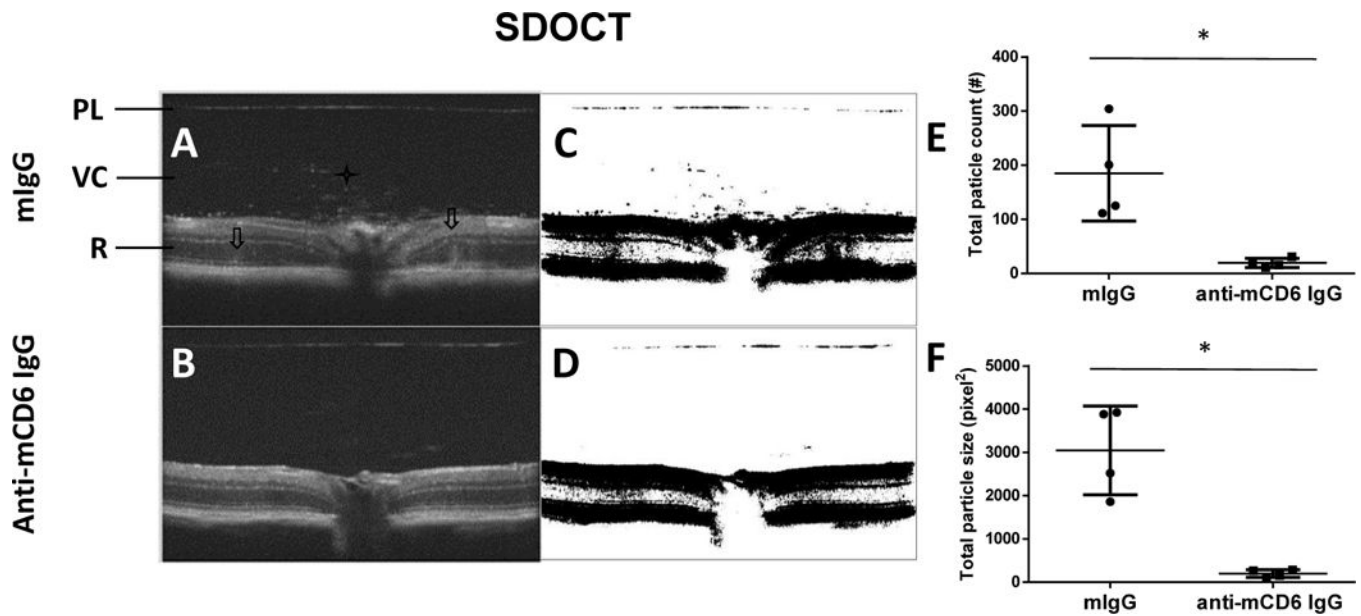


**Figure 5.**

Representative spectral-domain optical coherence tomography (SD-OCT) images and analysis in control and CD6 mAb-treated mice on Day 8 after transfer. A and B: SD-OCT images revealed more reflective foci (star) and retinal folds (arrows) in mouse IgG-treated mice, compared to CD6 mAb-treated mice. PL: posterior lens margin, VC: vitreous cavity, R: retina. C and D: Particles in the vitreous were assessed in SD-OCT images processed using ImageJ. E and F: Fewer total particles and reduced particle sizes were observed in the vitreous cavities of CD6 mAb-treated mice vs. control mice. Each dot represents one mouse. Data are shown as means  $\pm$  standard deviations. N=4. \*  $p < 0.05$ , Mann-Whitney test.



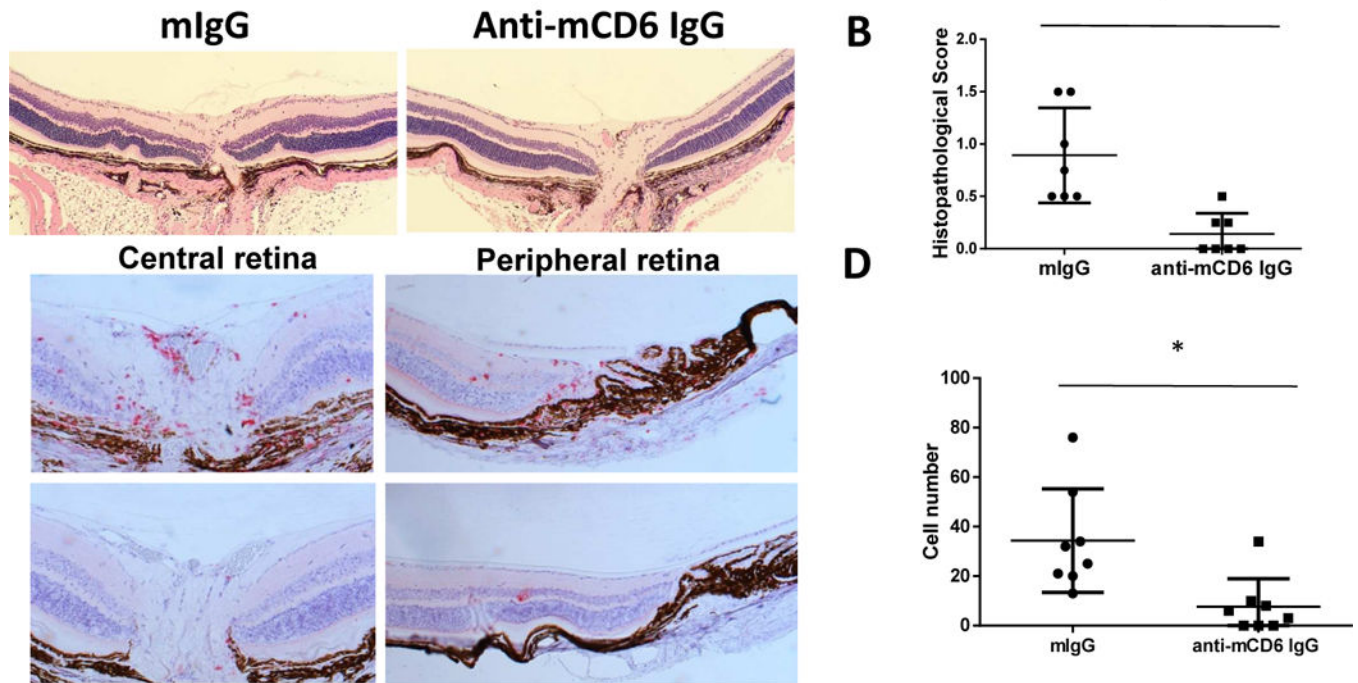


**Figure 6.**

A and B: Representative histopathological images and scores for control and CD6 mAb-treated mice with experimental autoimmune uveitis (EAU) on day 18 after the adoptive transfer of uveitogenic T cells. Mouse IgG-treated mice exhibited significant retinal folds, whereas the histopathological changes and scores were mitigated in CD6 mAb-treated mice. Data are shown as means  $\pm$  standard deviations (SD). N=7. \*  $p < 0.05$ , Mann-Whitney test. C and D: CD6 mAb-treated mice exhibited decreases in CD3+ T cell infiltration of both the central and peripheral retina. Data are shown as means  $\pm$  SD. Each dot represents the result from one eye. \*  $p < 0.05$ , Mann-Whitney test.